NMR Study of the Adsorption−Desorption Kinetics of Dissolved Tetraalanine in MCM-41 Mesoporous Material

Silvia Pizzanelli,[†,||] Shifi Kababya,[†] Veronica Frydman,[‡] Miron Landau,[§] and Shimon Vega*[,†]

Weizmann Institute of Science, Department of Chemical Physics and Chemical Research Support Unit, Rehovot 76100, Israel, and Ben-Gurion University of Negev, Department of Chemical Engineering, Beer-Sheva, Israel

Received: December 9, 2004; In Final Form: February 11, 2005

In this study we show how deuterium magic-angle spinning NMR spectroscopy can be used to investigate the adsorption−desorption kinetics of molecules in solution at surface−liquid interfaces. An aqueous solution of deuterium-labeled tetraalanine is inserted in the pores of MCM-41 mesoporous material, and its ^{2}H MAS NMR spectrum is measured as a function of temperature and fraction of filling of the pores. Prior to this study, the different types of water in MCM-41 are characterized as a function of water loading of the pores. Analysis of ^{2}H MAS sideband line shapes enabled the determination of the adsorption and desorption rates and the activation energies of desorption.

Introduction

The interaction of dissolved molecules with the surface of porous materials is an important factor in molecular transport, binding, selectivity, and chemical reactivity, such as in catalysis, chromatography, and slow drug release. The sizes and shapes of the pores, the binding properties of the surface, together with the shape and reactivity of the guest molecules determine the characteristics of molecular adsorption. Materials possessing regular arrays of uniform pore openings can provide a fairly homogeneous confined space, ideal to approach the problem of adsorption quantitatively. Experimental studies of the kinetics of molecular adsorption−desorption and the mobility of pure liquids in zeolites and mesoporous materials have been reported extensively.[1−6] On the other hand, to the best of our knowledge, similar studies are absent when the substrate molecules dissolved in a solvent are inserted in these porous structures.

In particular, we have chosen to characterize an aqueous solution of an oligopeptide embedded in a member of the M41S mesoporous materials, MCM-41. The adsorption of peptides on surfaces has been recognized to be critical in numerous fields such as biomaterials, biological separations, and biosensors. In this context, the exchange of proteins at the surface with molecules in the bulk has been investigated experimentally in the absence of a porous structure.[7,8] Studies concerning the adsorption of proteins on molecular sieves such as MCM-41 have also been reported, the problems addressed here being the efficiency of immobilization as a function of pH, concentration of the solution, and pore size,[9,10] and the catalytic activity in the case that the protein is an enzyme.[11−14]

The dynamics of the oligopeptides in the pores of mesoporous materials must be related to the dynamics of the solvent. Considerable interest has been focused on the issue of water in porous materials. In particular, NMR methods have mainly been used to characterize pore sizes by measuring freezing point depression and relaxation times, and water mobility by means of pulse field gradient methods and relaxation time measurements.[15]

In this publication we show how deuterium NMR can be used to study the adsorption−desorption dynamics of molecules at solvent−surface interfaces. In particular, ^{2}H MAS NMR[17] is applied and its spectra are analyzed to determine the adsorption−desorption rates of a deuterium-labeled tetraalanine salt (TA) at the surface of the pores of MCM-41. This technique is known to be a powerful tool for motional investigations of molecules,[16] ^{2}H line shapes being very sensitive to different types of reorientational motions at rates comparable to the strength of the deuterium quadrupolar frequencies. Low signal-to-noise prevents us from using static ^{2}H NMR.

This paper is organized as follows. First, details of the MCM-41 synthesis and the sample preparations are presented, together with the NMR parameters and details of the numerical analysis of the dynamic ^{2}H MAS NMR spectra. Then, the water content of MCM-41 is characterized using ^{1}H NMR. Different types of water and hydroxyl group protons in the channels are identified at various loading levels, and their mobility is characterized by temperature-dependent relaxation time measurements. With the additional help of ^{29}Si NMR and ^{2}H MAS NMR, the dynamics and the surface coverage of the silanol hydroxyl groups are determined. Knowing the surface coverage by the solvent and hydroxyl groups, the adsorption−desorption rates of the partially deuterated tetraalanine salt molecules at the surface are derived from dynamic ^{2}H magic-angle spinning (MAS) NMR spectra obtained as a function of water loading and temperature. The simple motional model making this derivation possible is discussed, and future extensions are suggested.

Experimental Section

Preparation of MCM-41. MCM-41 was prepared according to a procedure reported earlier.[17] A liquid mixture characterized by a composition SiO_2: 0.21 cetyltrimethylammonium chloride (CTAC): 0.21 Na_2O: 0.02 $(NH_4)_2O$: 89 H_2O was prepared by

* Corresponding author. E-mail: shimon.vega@weizmann.ac.il.
[†] Weizmann Institute of Science, Department of Chemical Physics.
[‡] Weizmann Institute of Science, Chemical Research Support Unit.
[§] Ben-Gurion University of Negev.
[||] Current address: Consiglio Nazionale delle Ricerche, Istituto per i Processi Chimico-Fisici, Area della Ricerca di Pisa, via G. Moruzzi 1, 56124 Pisa, Italy.

10.1021/jp044389e CCC: $30.25 © 2005 American Chemical Society
Published on Web 03/25/2005

TABLE 1: N_2 Adsorption, X-ray Diffraction, and SEM Data[a]

N_2 adsorption		XRD		SEM	
surface area ($m^2\ g^{-1}$)	1458	structure type	hexagonal	sample characteristics	curved rods with 0.1−0.3 μm diameter
pore volume ($cm^3\ g^{-1}$)	1.38	lattice space a_0 (nm)	4.73		
mean pore diameter (Å)	38				

[a] The wall thickness, calculated from the difference between the lattice space a_0 and the pore diameter, is equal to 9 Å.

combining two solutions. The first one was obtained by mixing 45.78 g of colloidal silica Ludox HS-30 (30% SiO_2, Aldrich) and 93.84 g of a 1 M aqueous solution of NaOH at 75 °C for 2 h. The second solution was prepared by combining 201.82 g of water, 60.76 g of a 25% aqueous solution of CTAC (Aldrich), and 2 mL of a 25% aqueous NH_4OH solution (Frutarom). The first solution was added dropwise to the second under stirring, and the mixture was further stirred vigorously in a plastic beaker for 1 h at room temperature. The resulting gel was transferred to a Teflon-coated autoclave and kept at 97 °C for 24 h. Then, the autoclave was cooled in an ice bath, and the pH was adjusted to 10.2 by adding 30% acetic acid. NaCl (8.34 g, Aldrich) was then added to the gel, followed by stirring at room temperature for 1 h. The heating at 97 °C, cooling, and pH adjustment (without NaCl addition) procedures were repeated three times. The resulting product was separated by suction filtration, dried at 120 °C for 2 h, and calcined in the air at 300 °C for 2 h and at 530 °C for 6 h.

Characterization of MCM-41. A N_2 adsorption−desorption isotherm was measured of the calcined sample, previously outgassed under vacuum at 250 °C, at liquid nitrogen temperature with a NOVA-2000 (Quantachrome, Version 7.01) apparatus. The surface area, pore volume, and pore diameter parameters were obtained from the isotherms, using the conventional BET and BJH methods.

X-ray powder diffraction data were collected on a diffractometer, consisting of a Rigaku (Japan) RU-100 X-ray generator that was operating at 50 kV and 150 mA, using a D-max/B goniometer. The radiation source was Cu Kα monochromatized with a graphite monochromator. The speed of acquisition was 0.1°/min with sampling intervals 0.05°.

SEM Pictures. Scanning electron microscopy (SEM) micrographs were taken from the MCM-41 sample with a JEM-5600 microscope of JEOL Co. The sample was coated by gold under vacuum for a few seconds, using an ion-sputtering system equipped with a magnetron electrode (Hitachi E-5100).

The properties of our MCM-41 sample are summarized in Table 1.

Preparation of Ala-3,3,3-d_3-Ala-Ala-Ala-3,3,3-d_3 (trifluoroacetate salt) (TA) and Ala-Ala-3,3,3-d_3-Ala-3,3,3-d_3-Ala (trifluoroacetate salt). All starting materials were of analytical grade and used without further purification. l-Alanine-3,3,3-d_3 was purchased from Isotec, Inc., and its free α-amino moiety was protected with a 9-fluorenylmethoxycarbonyl group (Fmoc) using standard procedures.[18] The peptides were synthesized manually using the standard solid-phase Fmoc strategy[19] on a 2-chlorotrityl chloride resin (200−400 mesh, 1.5 mmol/g, Novabiochem) and were characterized by mass spectrometry and amino acid analysis. No further purification of the peptides was necessary as ^{1}H NMR and mass spectrometry gave satisfactory spectra, and TLC in several solvents gave a single homogeneous spot.

MCM-41 Samples Loaded with an Aqueous Solution of Tetraalanine. The sample was prepared by adding MCM-41 (50 mg) to a solution of 30 mg of Ala-3,3,3-d_3-Ala-Ala-Ala-3,3,3-d_3 (trifluoroacetate salt) (or Ala-Ala-3,3,3-d_3-Ala-3,3,3-d_3-Ala (trifluoroacetate salt)) in water (1 mL) and stirring the suspension for 3 h at room temperature. The mixture was then filtered, and the residue washed with water and allowed to dry in the air for approximately 3 h. During drying, only the water at the external surfaces is evaporating, presumably leaving some very small amount of bound TA at these surfaces. The concentration of TA in the volume water in the pores of the fully loaded sample must therefore be very similar to that in the original TA solution.

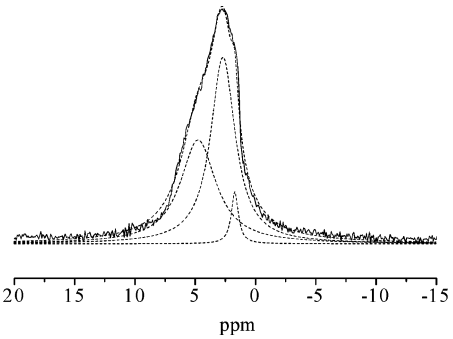

Figure 1. Room-temperature ^{1}H MAS spectrum of calcined MCM-41 before loading. The solid and dash lines represent the experimental spectrum and the components resulting from deconvolution, respectively.

To ensure that during this procedure the water indeed fills the MCM-41 pores and air bubbles do not hinder the water impregnation, ^{1}H NMR was used. The ^{1}H spectrum of a calcined MCM-41 sample, before loading, consists of a set of overlapping lines (see Figure 1). These lines are located at 1.7 (4%), 2.7 (53%), and 4.7(43%) ppm, showing that there is a significant amount of protons at 1.7 ppm belonging to the pore surface SiOH hydroxyl groups and at 2.7 ppm due to surface water (see paragraph 1.1 in the Results and Dicussion section for evidence for these assignments). Large portions of the channels of this sample must then be filled by air. Loading the sample with water resulted in the spectrum shown in the lower trace of Figure 2. This sample does not show any SiOH signals, even no signals that indicate exchange between water and −OH protons, and no air-filled pores can be present. Reintroduction of the SiOH lines is achieved after exposition of the loaded sample to vacuum for 1 day at 80 °C, as can be seen from the upper trace in Figure 2.

Another indication for the absence of air bubbles after water loading is the difference between the weight of the water-loaded sample before and after complete drying. This difference was equal (within 5%) to the weight of the amount of water that could fill the void space of the pores of our sample, as measured by N_2 adsorption measurements. Also, the presence of interparticle water can be excluded by the observation of supercooling of all the water contained in the sample in the temperature range −40 to 0 °C. In fact, no loss of signal was detected in the ^{1}H spectrum of the supercooled sample, which would have happened in the presence of frozen interparticle water, due to a dramatic increase of line width and a reduced transverse relaxation time.

To make samples with different amounts of adsorbed water, the as-prepared sample, packed in an uncapped MAS rotor, was

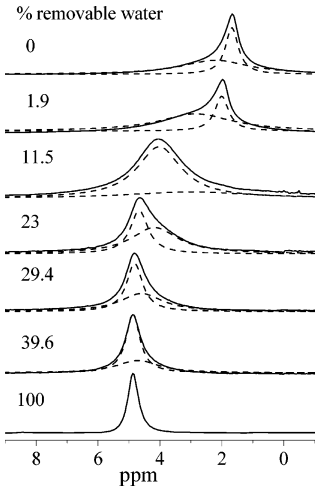

Figure 2. Room-temperature ^{1}H MAS spectra of MCM-41 as a function of the percentage of removable water. The solid and dash lines represent the experimental spectrum and the components resulting from deconvolution, respectively.

exposed to the vacuum of a turbomolecular pump for different durations. Before and after the pumping, the sample was weighed. The driest sample was obtained after exposition to the vacuum for 1 day at 80 °C. During this drying procedure, only water is removed from the sample, leaving the number of TA/nm^2 constant. This number is about equal to 50, relying on the fact that the concentration of TA in the fully loaded pores equals the concentration of the TA solution during sample loading.

XRD on the as-prepared sample showed that the structure of MCM-41 was not destroyed by this method of preparation.

MCM-41 Samples Loaded with D_2O. The sample containing only surface water was prepared by addition of MCM-41 (38 mg) to deuterated water (0.75 mL), the suspension being stirred for $^1/_2$ h at room temperature. The mixture was then filtered, and the residue was allowed to dry in the air for approximately 3 h. The sample, packed in an uncapped MAS rotor, was then exposed to the vacuum of a turbomolecular pump for a duration such that its ^{1}H MAS spectrum revealed the presence of only surface water.

The dry sample was prepared by exposing MCM-41 (13.6 mg) to the vacuum of a turbomolecular pump for 1 day at 80 °C. D_2O (4.7 mg) was then dropped on the MCM-41 and left in contact with it for 1 day. The sample was dried in the vacuum at 80 °C for 1 day.

NMR Measurements. ^{1}H and ^{2}H MAS experiments were carried out on a Bruker CXP 300 spectrometer operating at 300.13 and 46.07 MHz, respectively, equipped with a Bruker 4 mm MAS probe. The sample temperature was controlled employing a BVT 1000 variable-temperature unit, with a temperature stability of 1 K.

MAS NMR experiments on ^{1}H were carried out using a single 90° excitation pulse of 3 μs at a spinning frequency of 6 kHz and with a repetition delay between 3 and 10 s. ^{1}H spin−spin relaxation times were measured using the Hahn-echo sequence with a pulse spacing between 167 μs and 5 ms. ^{1}H spin−lattice relaxation times were measured using the standard inversion recovery sequence with a pulse spacing varying between 1 ms and 3 s.

Single pulse excitation has also been applied to obtain ^{2}H spectra; the 90° pulse being 3 μs, the spinning frequency 6 or 10 kHz, and the repetition delay 0.3 s. The free induction decay signals were Fourier transformed after a left shift of the data to the top of the first rotational echo position.

The sample temperature was calibrated following a procedure reported.[20] The temperature gradient over the sample, estimated from the line width of the ^{207}Pb spectrum of solid lead nitrate, was ±0.5°.

^{29}Si MAS experiments were carried out on a Bruker DSX 300 spectrometer operating at 59.6 MHz and equipped with a BL 4 mm Bruker MAS probe. The spinning frequency was 5 kHz, the 90° pulse was 5 μs, and the repetition delay was 600 s. Spectra were measured using the chemical shift echo (CSE) sequence (with $\tau = 200\ \mu$s). High-power proton decoupling was employed using the TPPM scheme with 80 kHz decoupling amplitude and $\Delta\varphi = \pm 17°$.

Simulations and Data Analysis. The dynamic ^{2}H MAS spectra were simulated employing a Fortran program written by Dr. Raphy Poupko.[21] Time domain signals were simulated by calculating the time evolution operator at successive times using Floquet theory.[22] The dimension of the Floquet matrix block for the site with a quadrupolar interaction different from zero was set to 31. The calculation was repeated for all the crystallites in the sample, and the combined signal was Fourier transformed to yield the frequency domain spectrum. Powder averaging was achieved by using the Conroy-Wolfsberg algorithm[23] considering a total of 1154 crystal orientations.

The evaluation of ^{1}H−^{1}H dipolar coupling constants from relative sideband intensities of the MAS spectra was performed using the SIMPSON program.[24]

All deconvolutions of the ^{1}H and ^{2}H spectra were performed using the dmfit program.[25]

Results and Discussion

1. Water Adsorption in MCM-41.

To study the surface adsorption−desorption dynamics of molecules in aqueous solution, it is first necessary to characterize the dynamic nature of the solvent molecules at the surface interface. In our case, this means that we have to verify the location and motional properties of the water molecules in the pores of our MCM-41 samples as a function of solvent-loading. Here this is done with the help of ^{1}H and ^{2}H MAS NMR measurements on samples with varying loading levels of H_2O and D_2O at different temperatures.

1.1. Characterization of Water as a Function of Loading.

To verify the pore filling and the surface coverage, we studied first the changes in the proton spectra of a H_2O-loaded MCM sample as a function of the percentage of removable water at room temperature. The amount of removable water was determined by the difference between the weight of the sample at a given hydration level and its weight when the maximum amount of water was removed.

A series of ^{1}H MAS spectra of this study is shown in Figure 2. The analysis of the spectra reveals the presence of different types of protons. At high loadings, one peak at a chemical shift of about 4.8 ppm and with a line width of 0.3−0.7 ppm is observed. On the basis of this chemical shift value, this peak can be attributed to water molecules filling the volume of the channels. In fact, this chemical shift is close to the value of normal bulk water. This value is a result of a weighted average of the proton shifts of SiOH (between 2.7 and 1.7 ppm) and bulk water protons, which shows that at high loading levels the fraction of silanol protons is much smaller than those of the water. The absence of a separate peak in the spectrum from the SiOH protons of the siliceous matrix[26] indicates that essentially all the silanol protons exchange with water protons, thus are located at the water-accessible surface of the MCM-41 sample.

At a loading of about 60% removable water, an additional peak appears, characterized by a chemical shift lower than 4.8 ppm. The two peaks stay present simultaneously until approximately 80% of the water has been removed. At that level of loading, the 4.8 ppm peak disappears. The new peak is broad (1.2−1.8 ppm) and tends to shift upfield (from 4.7 to 3.8 ppm) when the moisture level decreases. It can be attributed to water protons distributed on the surface of the channels, exchanging with the silanol protons. Their water molecules form surface layers with average thicknesses that decrease slightly during sample drying.

The simultaneous presence of volume and surface water peaks in the 60−20% removable-water range indicates that the water molecules in the different environments do not exchange. This type of water distribution has already been observed for SBA and MCM-41 samples with channels that were partially filled and partially covered with thin surface layers.[27,28] The actual sizes of the surface areas covered by water layers can not be determined by our experiments.

To get a better insight into the dynamic nature of the water in the pores, Hahn-echo experiments were done on a sample that was reloaded with water after evacuation and had a water content of 39.6%. At this loading level, the volume and surface water peaks can be clearly distinguished. The integrated signal intensities of both lines decay exponentially as a function of the echo-delay time. The echo decay of the volume water corresponds to an intrinsic line width of 120 Hz, which compares well with a line width of 160 Hz measured from the volume water peak in the spectrum, not showing any significant source of spectral inhomogeneity for these protons. On the other hand, the echo-decay of the surface water corresponds to a line width of 230 Hz, which is significantly smaller than the corresponding actual line width of 360 Hz. This is evidence for some inhomogeneous broadening that must be due to chemical shift dispersion, induced by local differences in the water coverage of the surface. The exponential decay of the echo intensities shows that the small differences in surface coverage do not influence the T_2 relaxation time.

At 10% removable water, another peak appears with a chemical shift of 3.0 ppm. This peak (moving from 3.0 to 2.7 ppm) with a line width of about 800 Hz is present also at the lowest loading levels, together with a relatively narrow peak (between 2 and 1.7 ppm) with a width of 150 Hz. These two resonances, which have been observed as well in silica gel,[26] were attributed to hydrogen-bonded silanols and "isolated" (non-hydrogen-bonded) silanols, respectively. In the literature, the existence of these two types of silanols has been proved for MCM-41 by means of microcalorimetry and IR.[29,30] The width of the 3 ppm peak has been ascribed to a distribution of chemical shifts, which should reflect a variety of hydrogen-bonding distances.[18]

In our driest sample, both peaks show rather weak sidebands, indicating some residual homonuclear $^1H-^1H$ dipolar interactions. Assuming a two-proton model system, the sideband intensities correspond to dipolar coupling constants of about 5 kHz (corresponding to an average distance of about 2.9 Å) and 1.5 kHz (with an average distance of about 4.3 Å) for the 2.7 and 1.7 ppm peaks, respectively. This difference indicates a closer proximity of neighboring hydrogens at the surface for the hydrogen-bonded silanols than for the isolated silanols.

The integrated intensity of each proton spectrum showed a linear relationship to the weight of removable water in the sample. From this dependence and the integrated intensity of the driest sample we can estimate, taking into account the inner surface area per gram (1458 $m^2\ g^{-1}$), that in this sample there are 4.5 ± 0.5 protons per 1 nm^2 present on the surface of the pores. The uncertainty in this number is due to the inaccuracy of the integrated signal intensity. When all these protons would belong to SiOH groups, this value seems to be rather high, compared with values reported in the literature for MCM-41.[3,29,31] This suggests that part of the residual protons still belong to water-like molecules that act as a proton donor of the hydrogen-bonded SiOH group.

Assuming that all lines between 4.8 and 3.8 ppm correspond to protons exchanging between free water and the protons of the two types of hydroxyl groups at the surface, we can make a quantitative estimate of the ratio between the number of volume water or surface water protons and the number of protons of the isolated and hydrogen-bonded silanol groups. Taking for the chemical shifts of the two types of protons the values 5 and 2.3 ppm (i.e., the average ppm value of the two lines at respectively 2.7 and 1.7 ppm with relative intensities 3:2), the proton ratio in the sample with volume water is 12.5 and in the samples with surface water it varies from 8.0 to 1.2. Using the facts that the number of protons at the two types of hydroxyl sites is about 4.5 per 1 nm^2 and that the number of actual SiOH groups per 1 nm^2 is about 2 (see below), the number of H_2O molecules for each surface SiOH is for the volume water about 14.7 and for the surface water it varies from 9.6 to 2.0. The number 14.7, which corresponds to 29.4 water molecules/nm^2 for a silanol surface density of 2 SiOH/nm^2, compares well with the number of 31.4 water molecules/nm^2 that is calculated for fully loaded pores by considering a pore diameter of 3.8 nm and a water density of 1 g cm^{-3}. The number of water molecules for the surface water varies according to the average thickness of the water layers at the surface.

To verify the density of hydroxyl groups at the inner surfaces of the channels, ^{29}Si NMR single pulse experiments were performed to determine the Q^4/Q^3 ratio (i.e., $(SiO)_4Si/(SiO)_3SiOH$) of our MCM-41 sample. This ratio for the driest sample was found to be about equal to 2. Taking the weight and the surface area of the sample into account, this value corresponds to about 2 SiOH/nm^2. In this estimation, all the silanols are assumed to be on the surface, as indicated by our ^1H NMR data. This value, which is comparable to values reported in the literature,[29,31] is smaller than the number of protons/nm^2 obtained by means of our ^1H NMR from the driest sample. This difference is indicative of the presence of residual water in the hydrogen-bonded silanol networks, as was already mentioned above.

At this stage of the discussion, we can conclude that we can distinguish four types of protons in our systems: (i) protons belonging to volume water, (ii) protons belonging to surface water, (iii) protons participating in the hydrogen bonding of nonremovable silanol networks (SiOH(II)), and (iv) protons of isolated non-hydrogen-bonded silanols (SiOH(I)). The relative integrated intensities of the lines corresponding to the four types of protons as a function of removable water are shown in Figure 3.

1.2. Mobility of the Water in MCM-41.

The reorientational dynamics of the water molecules is characterized by an overall correlation time of motion that can be determined by measuring the temperature dependence of the proton spin−lattice relaxation time. Figure 4 shows the ^1H spin−lattice relaxation times T_1, obtained by inversion recovery experiments, of a sample containing approximately equal amounts of volume and surface water (with 39.6% removable water) in the temperature range of 235−295 K. Both peak

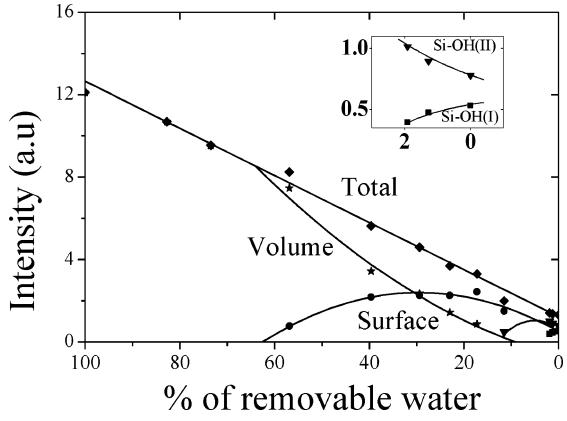

Figure 3. The values of the integrated signal intensities of the lines corresponding to the four types of protons in a MCM-41 sample as a function of the percentage of removable water. The total proton signal intensity (◆), the signal intensity from the volume water (★), the surface water (●), the SiOH's of type (iii) (▼), and SiOH's of type (iv) (■) are shown.

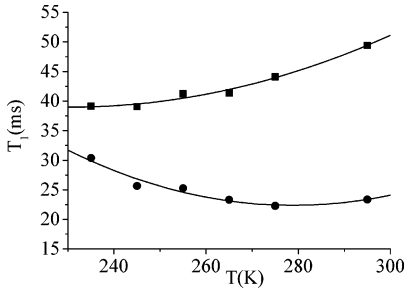

Figure 4. ^{1}H spin−lattice T_1 relaxation times of the volume (■) and surface (●) water in a sample with 39.6% removable water, as a function of temperature. The lines in the figure are there to guide the eye.

intensities decayed exponentially as a function of recovery time with slightly different T_1 values: between 40 and 50 ms for the volume water and between 20 and 30 ms for the surface water. These values are close to values already reported for similar systems.[32,33] Although the temperature dependence is rather weak in the range investigated, it can be seen in Figure 4 that the temperature-dependent T_1 values show minima, centered at about 240 K in the case of the volume water and at 275 K for the surface water.

The T_1 values can be analyzed using the theory of Bloembergen et al.[34] The longitudinal relaxation rate $1/T_1$ of a system of identical nuclei subjected to a dipolar interaction and undergoing isotropic reorientational Brownian motion can be expressed as

$$\frac{1}{T_1} = K\tau_c\left(\frac{1}{1+\omega_0^2\tau_c^2} + \frac{4}{1+4\omega_0^2\tau_c^2}\right) \qquad (1)$$

where τ_c represents the overall correlation time of motion and ω_0 is the Larmor frequency. The parameter K includes a number of fundamental physical constants and a geometrical factor related to the distance between the interacting nuclei. The inverse of the correlation time τ_c, characterizing the overall motion of the water molecules, can be expressed as the sum of the inverse of the correlation times associated with the diffusion and rotation motion of the spin pairs.[35] In this description, the exchange of the water protons with the surface protons should be considered as a source for lowering the overall correlation time τ_c. Considering eq 1 and adjusting the minima in Figure 4 to the correlation time value $\tau_c = 0.62/\omega_0 = 3.2 \times 10^{-10}$ s, the actual T_1 values at these minima result in two K prefactors: 6.0×10^{10} s^{-2} for the surface water and 3.3×10^{10} s^{-2} for the volume water. These K values are of the same order of magnitude as K values reported in the literature.[35] The difference in the two values must be attributed to differences in the hydrogen-bonding characteristics and interactions with the surface of the volume and surface water.

The order of magnitude of the effective correlation times ($\tau_c \approx 10^{-10}$ s) in our MCM-41 sample is lower than of bulk water, with a typical correlation time of the order of $\sim 10^{-12}$ s. Evidence for a lowering of mobility of water in MCM-41 has already been provided by other spectroscopic methods, like neutron scattering[36] and NMR using both pulse field gradient[37] and Carr-Purcell-Meiboom-Gill[35] techniques and ^{2}H NMR.[38,39]

Before studying the mobility of the surface hydroxyl groups we should have a look at the actual values of the water chemical shifts as a function of temperature in order to further characterize the nature of the volume and surface water. To do so we measured the chemical shift values of the sample loaded with 39.6% removable water in the temperature range 235−295 K. Upon cooling, the volume water chemical shift increases by about 0.5 ppm with respect to the value at room temperature, while the chemical shift of the surface water decreases insignificantly (∼0.1 ppm). In addition, no significant temperature dependence was observed for the peak positions of the driest sample.

Data concerning the chemical shifts of the surface water and of the silanols as a function of temperature were not found in the literature. However, studies on the structure of water in MCM-41 in the liquid and supercooled states have been reported.[40] In particular, XRD measurements have shown that fully filled samples tend to form more tetrahedral-like hydrogen-bonded water structures at subzero temperatures, whereas no significant structural changes were observed for a partially filled sample.[41] Our results seem to be consistent with these findings indicating a similar behavior of the water in our samples.

1.3. Mobility of the Hydrogen-Bonded and Isolated Silanols.

To obtain additional information on the dynamics of the protons at the surface of the pores, we performed room-temperature ^{2}H MAS NMR experiments on MCM-41 samples loaded with different amounts of D_2O. Two samples were prepared, one containing only surface D_2O and one a dry sample. The deuterium spectrum of the former (not shown) showed a single line without any sidebands, indicating that the surface water reorients isotropically. On the other hand, the spectrum of the dry sample showed a broad peak, constituting 15% of the total signal intensity, without sidebands, together with two sideband patterns characterized by two different quadrupolar constants, each contributing approximately the same 42% to the integrated intensity (Figure 5). The two sideband spectra are shifted with respect to each other by ∼1 ppm and have different line widths (50 and 150 Hz). These patterns must be attributed to the "isolated" silanol groups (type SiOH(I)) and to the hydrogen-bonded silanols (type SiOH(II)). In fact, the difference in the chemical shift values compares well with the one observed in the ^{1}H spectrum for these two types of protons. The broad single peak (Figure 5, trace d), with an intermediate chemical shift between the center lines of the two quadrupolar sideband patterns, must then be attributed to some exchanging water molecules between the two types of SiOH protons.

The sideband pattern of the "isolated" silanols can be interpreted as resulting from the rotation of the OD bond about an axis, defined by the SiO bond. The spectrum can be reproduced assuming a static quadrupolar coupling constant of

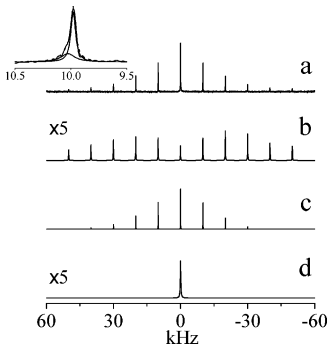

Figure 5. Room-temperature ^{2}H MAS spectrum of a sample loaded with D_2O and dried (a). Deconvolution of the spectrum results in two MAS sideband patterns corresponding to the hydrogen-bonded silanols SiOH(II) (b) and the isolated silanols SiOH(II) (c). For an interpretation of the signal shown in (d), see the text. The inset shows an expansion of one of the first-order sidebands.

200 kHz,[42] with an angle between the axis of rotation and the OD direction of both 47 ± 2° and 63 ± 2°. Values close to both these tilt angles of the OD bond have been reported in the literature.[3,43] The hydrogen-bonded silanol sideband pattern is much wider than the former and reveals the presence of some residual anisotropic motion, as the full static tensor is only partially reduced. This is an indication of directional order of the deuterium quadrupolar tensors of the nonremovable silanol networks imposed by the surface.

Up to this point we have characterized the dynamic nature of the four types of protons of the water and silanols located in the pores of MCM-41. The different types of protons coexist in the same sample and at different water loading levels. (i) The volume water has an overall correlation time longer than that of bulk water and can be removed from the sample. (ii) The surface water, showing even a longer correlation time due to its fractional binding to the surface, is associated with thin layers of water exchanging with the protons of the silanols. This type of water can be observed only at low loading levels and can also be removed from the sample. (iii−vi) Finally, the two types of silanol protons SiOH(I) and SiOH(II) are bound to the surfaces and thus cannot be removed and show a strong anisotropy in their orientational motion.

2. Adsorption and Desorption Rates of the Tetraalanine (TA) Salts in MCM-41.

After characterizing the two types of water and two types of silanol groups present in our samples, we will now study the adsorption and desorption of dissolved TA molecules at the MCM-41 inner-surface, expecting that the adsorption−desorption kinetics will change with the water content. In the following, we show how the adsorption and desorption rates of these TA molecules, deuterated at their outer methyl groups, can be determined using ^{2}H MAS NMR.

These TA molecules, dissolved in water inside the channels of the MCM-41 mesoporous material, are expected to reorient freely, constantly changing their conformation. Only surface binding effects will disturb this dynamics. This picture is based on the general belief that the individual residues of short peptides can sample the entire allowed regions of the Ramachandran space.[44] Although some recent experimental work shows the existence of a limited number of conformers for some oligopeptides in water,[45,46] it will be shown that on the NMR time scale our data seem to be consistent with the former picture.

2.1. TA Mobility as a Function of Water Loading.

Figure 6 shows a series of ^{2}H MAS spectra of TA inside a MCM-41 sample recorded at room temperature and measured

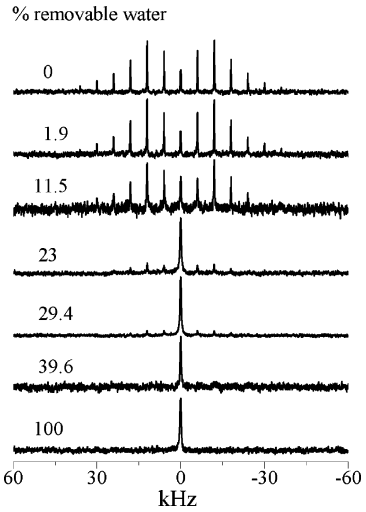

Figure 6. Room-temperature ^{2}H MAS spectra of the TA molecules in MCM-41 as a function of the percentage of removable water.

as a function of the percentage of removable water. At the highest moisture levels, a peak with a width of ∼400 Hz and without sidebands is present originating from the outer methyl groups of TA. This single line is an indication of an isotropic motion of the TA peptide segments in solution. Lowering the water content the spectrum exhibits additional solid sideband patterns. At the lowest water loading, the sideband pattern is characterized by an effective quadrupolar coupling constant e^2qQ/h of 51 kHz and a line width of all bands of ∼100 Hz. In fact, this constant is about one-third of a typical coupling constant for a rigid CD deuteron,[47,48] as expected for nuclei experiencing a fast exchage between three sites of tetrahedral or slightly distorted tetrahedral geometries.[49] The fact that we observe a sideband pattern that can be analyzed by a single quadrupolar constant indicates that the methyl groups of TA, which are located at the two extremes of the molecule, are simultaneously fixed in space or undergo some very small directional fluctuations. The motional restriction of the TA molecules at the surface leading to these sidebands can thus be solely described by a single fast rotation of the methyl groups about their C_3 symmetry axis, the backbone of the TA molecules being fixed in space. The results of Figure 6 thus mean that we must at least distinguish between two types of TA molecule: those with isotropically moving peptide segments and those that are bound to the surface of the MCM-41 channels and allow only internal methyl rotations.

In this study, we did not attempt to characterize the details of the binding of TA to the surface itself or their exact reorientational and conformational motion in solution. This will be approached in a future study using ^{13}C and ^{1}H MAS NMR.

A careful inspection of the spectra at intermediate moisture levels reveals that the ^{2}H signals are in fact composed of narrow as well as broad components, each one characterized by its own sidebands. This suggests that, at a given loading, different TA molecules undergo different dynamic processes, which must be ascribed to the fact that they experience different environments, in agreement with the heterogeneous distribution of the water in the channels proposed before. Thus three types of subspectra with varying relative intensities can be recognized: a narrow single line, a narrow line sideband pattern with a quadrupole coupling constant of 51 kHz, and a broad line sideband pattern. The narrow components of the spectra must be due to molecules that move completely free in solution or that are fixed to the inner- and outer-pore surfaces. The broad spectrum, characterized at ambient temperature by a line width of approximately 1

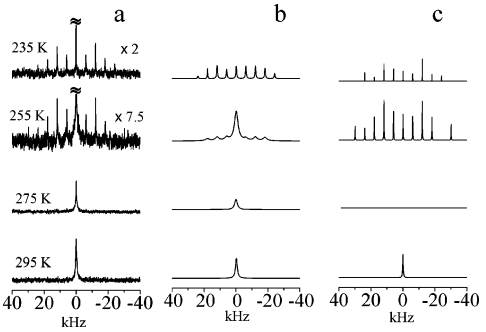

Figure 7. ^{2}H MAS spectra of TA in a MCM-41 sample loaded with volume water as a function of temperature (a). Columns (b) and (c) show, respectively, the broad and narrow sideband patterns, obtained from the deconvolution of the spectra. The sharp center component present at temperatures lower than 295 K is not shown.

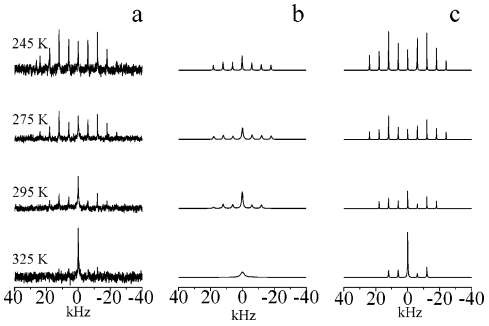

Figure 8. ^{2}H MAS spectra of TA in a MCM-41 sample loaded with only surface water as a function of temperature (a). Columns (b) and (c) show, respectively, the broad and narrow sideband patterns, obtained from the deconvolution of the spectra.

kHz, should correspond to molecules in the channels. This spectrum is indicative of a dynamic process involving the slowing down of the motion of TA in the pores. In the following we will investigate the nature of this dynamic process.

A similar overall behavior of the deuterium spectra was observed from a MCM-41 sample loaded with TA molecules, with their two inner methyl groups deuterated. Because of the similarity between the results from this sample and from the former one, no spectra are shown here and no separate discussion is necessary. We should only mention that the immobile molecules again exhibit sideband patterns with a quadrupolar coupling constant of 51 kHz, strongly suggesting that the backbones of the TA molecules are about fixed in the pores.

2.2. TA Mobility as a Function of Temperature.

To get an insight into the nature of the process leading to the slowing down of the molecular motion as a function of loading level, a temperature study of the TA ^{2}H spectra at two different water loadings was undertaken. In particular, a sample containing mainly volume water and a sample with only surface water were examined as a function of temperature.

A series of ^{2}H MAS spectra of these two samples, recorded at a spinning frequency of 6 kHz, are shown in Figures 7 and 8. Traces (b) and (c) in these figures represent, respectively, the broad and narrow sideband patterns obtained from Lorentzian line deconvolutions of the spectra. Not shown are the residual single narrow lines at the center of the spectra. The main contribution to the signal in both samples is the broad component (80−90% for TA dissolved in volume water and 70−80% for TA dissolved in surface water), except for the spectrum of the surface water sample at the lowest temperature, where the broad contribution is only about 40%. These results indicate that the largest part of the TA molecules is subject to an exchange process that can manifest itself in changes in the ^{2}H spectra in the temperature range 275−245 K. As will be shown below, the experimental results show that all exchanging molecules in each sample behave about the same, excluding a strong inhomogeneous distribution of the water in the channels.

The overall line shape of the broad sideband patterns is strongly dependent on temperature in both samples. In the volume water sample, a single peak characterized by a width of 1.3 kHz at room temperature tends to broaden and to show sidebands upon cooling, reaching a maximum line width of 2.7 kHz at 255 K and becoming a relatively sharp sideband pattern at 235 K. The surface water sample shows a broad peak of 2.6 kHz at the highest temperature 325 K that tends to sharpen and to show sidebands with increasing intensities on lowering the temperature. A quantitative analysis of these spectra is given in the next section.

The narrow parts of the spectra are represented by either a single peak at the highest temperature or by a static MAS pattern at the lowest temperatures. A combination of the two can be observed at 325 and 295 K in the sample with surface water. It is not clear why this is not detected at 275 K in the sample with volume water. As mentioned above, these narrow signals are indicative of free-moving or fixed molecules and could correlated to TA molecules located in extra porous spaces and in regions at the edge of the channels, where the relative amount of water can differ significantly from that in the pores. The sharp peak without sidebands, detected in the volume water sample and composing ∼10% of the total signal at temperatures below 295 K, is then due to TA molecules in regions outside the pores. In fact, this peak was not observed in the other sample, for which extra porous water, being less tightly bound to the surface, had been removed. Nitrogen adsorption data has shown that the MCM-41 samples are characterized by relatively large external surface areas, up to 10% of the total detected surface.[17] We did not attempt to verify these conjectures any further.

2.3. Dynamic ^{2}H MAS NMR Spectra.

To analyze the dynamic ^{2}H spectra, we suggest a model that can simulate the line shapes of the broad component observed in both samples. The exchange process of the methyl deuterons of the TA molecules is assumed to take place between two sites with well-defined quadrupolar frequencies. These two sites are chosen according to the two types of narrow spectra observed in the samples: one site, corresponding to molecules fixed at the surface with a symmetric quadrupolar constant of 51 kHz, and the other corresponding to TA molecules free-rotating in solution with no quadrupolar coupling constant. The hypothesis of the existence of a site where TA molecules move isotropically, even when only surface water is present, is based on the fact that tetraalanine is expected to be highly flexible,[44] and therefore able to assume nonelongated conformations, which require relatively small amounts of water for their reorientation.

The parameters necessary to quantify the exchange model are the relative populations p_b and p_f of surface-bound (site *b*) and free-reorienting (site *f*) molecules and an exchange rate K parameter, which is defined as

$$K = k_{bf}p_b + k_{fb}p_f \tag{2}$$

where k_{bf} and k_{fb} are the jump rates per molecule from site *b* to *f*, and vice versa, respectively. These rates can be expressed as a function of K and p_b, assuming that the system is in a stationary state:

$$k_{bf} = \frac{K}{2p_b} \tag{3}$$

and

$$k_{fb} = \frac{K}{2(1 - p_b)} \tag{4}$$

A set of ^{2}H MAS spectra were calculated for the two-site exchange model for a spinning speed of 6 kHz and for different K and p_b values, using a Floquet theory-based simulation program. Results are shown in Figure 9, where it can be seen that the overall line shape of the ^{2}H spectrum is very sensitive to both parameters. For low values of K, each spectrum is a superposition of the spectra of the individual sites. When K increases for a fixed relative population p_b, broadening of the lines composing the spectrum occurs until a maximum is reached for K of the order of the quadrupolar constant. After that, narrowing takes place and an averaged single sideband pattern develops.

On the basis of this model, the experimental broad parts of the temperature-dependent signals shown in Figures 7 and 8 were simulated. An interval of possible values of K and p_b was identified simply by comparing an experimental spectrum with the series of simulated ones shown in Figure 9. This range was then refined by simulating addition spectra for K and p_b values within the interval. The procedure was repeated until the line width and the fraction of the central band intensity of the calculated spectrum agreed with those of the experimental one within 10%. Comparisons between the experimental and simulated spectra are shown in Figures 10 and 11. The K and p_b parameters used for the simulations are summarized in Table 2. A line broadening of 100 Hz was imposed on all simulated spectra. No additional line broadening was performed during the Fourier transformation of the experimental data.

For both samples, an increase in the population of the surface site p_b occurs upon cooling. In addition, the coverage of the surface at a given temperature is always higher for molecules in surface water, and the population range spanned by the two samples differs: while in the volume water essentially the whole population range is covered, in the surface water case a significant portion of molecules is still bound even at 325 K.

The exchange rate parameter K tends to decrease upon cooling and in the surface water it is smaller than in the volume water, at the same temperatures.

We should mention that the derived values for K and p_b can exert errors that are mainly caused by low signal-to-noise ratios of the spectra. Another source of some error is the uncertainty about the natural line width for each site at the temperatures of detection.

2.4. Temperature Dependence of the Adsorption and Desorption Rates.

To simultaneously present the results for the two samples as a function of the population p_b and exchange parameter K, two contour plots, one for the simulated line width and one for the simulated relative centerband intensity of the spectrum as a function of these two parameters, were calculated and superimposed. The result is shown in Figure 12. In the calculation of the spectra for the construction of the contour plots, no line broadening was imposed. The line width, *lw*, and the fraction of central band intensity, *ci*, were obtained after deconvolution of the calculated spectra with Lorentzian line shapes. This is an approximation since the line shapes of the sidebands are not necessarily Lorentzian.[22]

From the shapes of Figure 12, it is clear that each data set {*lw*,*ci*} corresponds to two positions on the combined contour plot. This ambiguity can be generally overcome by comparing the experimental spectrum with parameters {*lw*,*ci*} with the line shapes calculated from the two corresponding parameters {p_b, K} resulting in the same {*lw*,*ci*}. In addition, it is physically reasonable to expect that the rate constant parameter K decreases when the temperature is lowered, and the population p_b of the bound molecules increases. This imposes {p_b, K} pathways on the contour moving from right to left, and from bottom to top upon cooling.

The dots placed on the contours of Figure 12 represent the spectra of samples with volume and surface water at different temperatures. From this plot the trends of p_b and K are clear: the fraction of molecules bound to the surface tends to increase and the kinetics of the adsorption−desorption tends to become slower upon cooling. For the sample containing volume water, the trend of p_b could be interpreted considering that hydrogen bonding among water molecules is strengthened compared with the hydration of TA with decreasing temperature, which would result in the tendency of TA to be expelled to the region close to the wall. Instead of the fractional population p_b and the rate parameter K, from now on we will consider the two rate constants, k_{bf} for desorption and k_{fb} for adsorption, more treatable from a physical point of view. These rates can be derived from the rate parameter K and the relative population p_b, according to eqs 3 and 4.

A discussion of this temperature dependence and its physical significance is presented in the following.

2.5. Discussion of the Results.

The adsorption rate per molecule is governed by the rate of arrival of a molecule at the surface and by its sticking probability, which expresses the fraction of arrivals at binding sites on the surface that lead successfully to adsorption. The rate of arrival is determined by diffusion, while the sticking probability is proportional to the fraction of vacant binding sites, according to Langmuir's model.[50] Another factor influencing this probability is related to the orientation and the conformation of the molecules with respect to the surface, as only certain functional groups are able to bind.

Thus the adsorption mechanism is generally depicted as a combination of processes: as the molecule approaches the surface by diffusion, its energy falls as it becomes physisorbed to some precursor sites on the surface before its binding site finds itself in the right orientation and at the appropriate position on the surface to chemisorb. In the physisorbed state van der Waals interactions are involved, while during chemisorption at least one chemical or hydrogen bond is formed. When diffusion does not limit adsorption, because of small amounts of solvent, only molecular reorientational motion should be considered.

In our case, the surface coverage is always low. Although we do not have any evidence on the nature of the surface binding site itself, it is reasonable to assume that the hydroxyl groups are involved. The surface area available to a single TA molecule is roughly 50 nm^2, if the concentration of the solution in the pores is assumed equal to that used in the preparation of the sample. On this area, the number of SiOH groups is ∼100, which is calculated by taking into account the density of silanols derived by ^{29}Si NMR. A TA molecule, even in the all-trans conformation with a length of approximately 15 Å, will need only a limited number of SiOH groups, leaving most of them free.

If the adsorption rate is dependent on the diffusion constant of the molecules, the rate k_{fb} should be affected by its

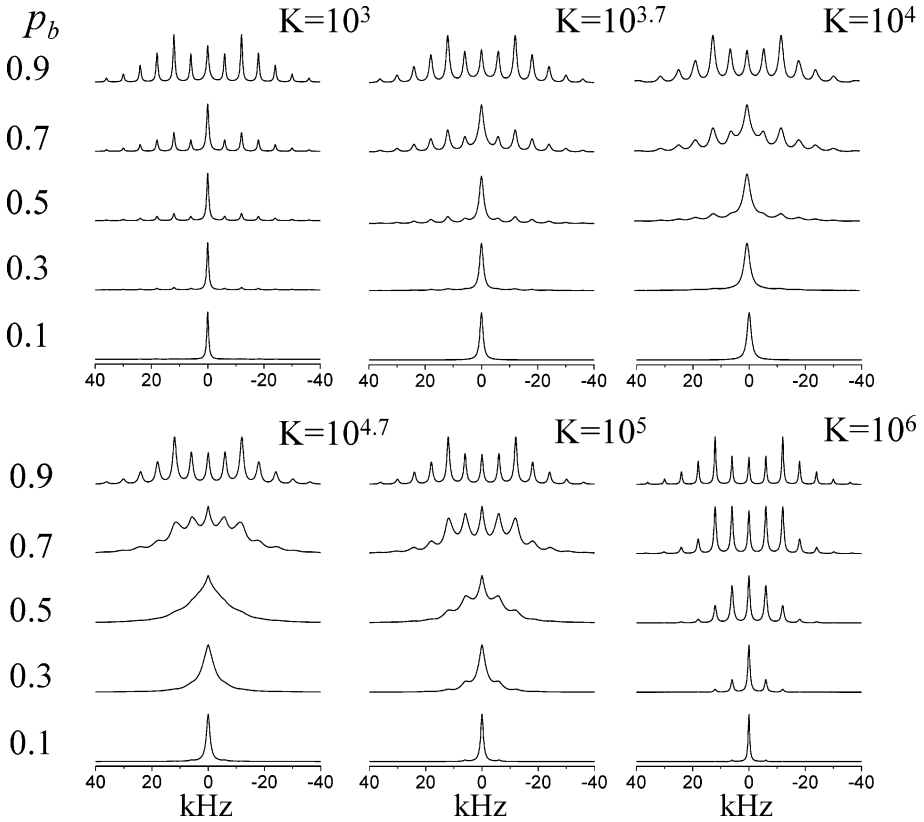

Figure 9. Spectra calculated for different values of the exchange parameter K and the relative population of the surface site p_b. The spinning speed was set to 6 kHz and the line broadening to 600 Hz.

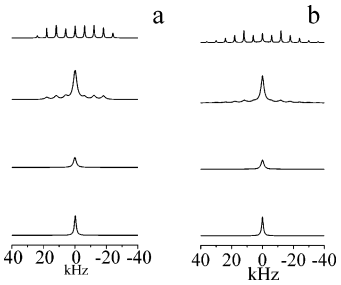

Figure 10. Comparison between the broad components of the signals (a), obtained after deconvolution of the experimental ^{2}H MAS spectra of TA in the sample with volume water at different temperatures, and the spectra (b) calculated according to the two-site model.

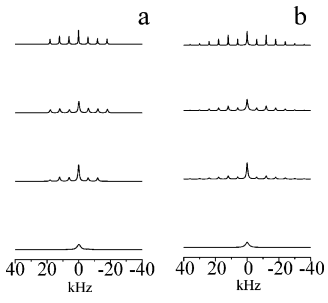

Figure 11. Comparison between the broad component of the signal (a), obtained after deconvolution of each experimental ^{2}H MAS spectra of TA in the sample with surface water at different temperatures and the spectra (b) calculated according to the two-site model.

temperature dependence. However, in our case we expect that the diffusion of TA molecules does not change much with temperature, as the correlation times of the water, which are related to the diffusion of the solute, do not show a strong temperature dependence (see paragraph 1.2).

TABLE 2: Values of p_b and log K Used in the Simulation of the Broad Component of the Spectra of the Samples with Volume and Surface Water at Different Temperatures (Figures 10 and 11)

sample	T (K)	p_b	log K
TA in volume water	235	0.89	3.4
	255	0.44	4.0
	275	0.22	4.1
	295	0.10	4.5
TA in surface water	245	0.78	3.0
	275	0.67	3.5
	295	0.56	3.5
	325	0.22	4.2

If this is the case, only the temperature dependences of reorientational and conformational motions will possibly affect the temperature dependence of the adsorption rate. These dependences may be rather complicated as different dynamic processes may be involved. Combining all the arguments about the surface coverage, diffusion dependence, and molecular reorientation, we should not expect the adsorption rate to follow a simple Arrhenius type of temperature dependence.

Plots of the logarithm of k_{fb} as a function of $1/T$ for the samples with volume and surface water are shown in Figure 13. Although straight lines through the experimental points show a very weak temperature dependence, the quality of the data does not allow any conclusion about this actual dependence.

The difference between the overall values of the rate constants in the two samples should result from the difference in their water content. While in the sample with volume water the diffusion of the molecules in the water can limit the rate of adsorption, in the sample containing surface water the constant proximity of the TA molecules to the surface rules out this effect. We should therefore expect that k_{fb} will be higher in the latter sample than in the former, when we assume that the

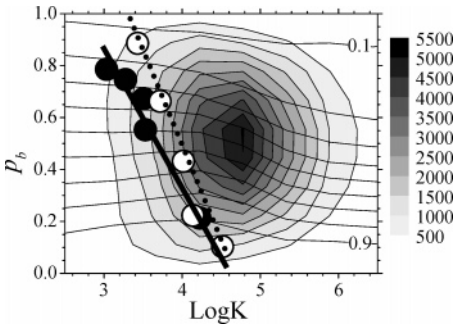

Figure 12. The closed contour plot of the line width of the sideband in the MAS spectra calculated as a function of the relative population p_b and the logarithm of K for the two-site model. The horizontal lines represent the contours of the fractional intensity of centerbands of the same MAS spectra. The number of calculated spectra used to build this combined contour plot was 60, and the number of points constituting each grid was 100 (10 × 10). The dots represent the experimental data obtained from the broad components of the ^{2}H MAS spectra of TA, recorded at different temperatures in samples with volume (○) and surface (●) water. The temperatures are decreasing from the bottom to the top. Their values are 295, 275, 255, 245, and 235 K for the volume sample, and 325, 295, 275, 255, and 245 K for the surface sample.

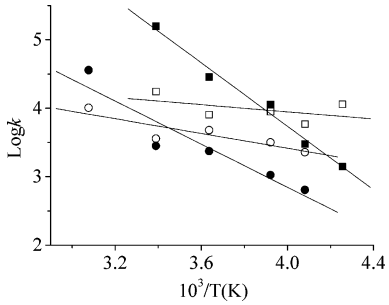

Figure 13. The dependences of log k_{fb} and log k_{bf} on $10^3/T$ for samples with volume (■ and □, respectively) and surface (● and ○, respectively) water. The solid lines represent linear fits through each data set.

reorientational dynamics is the same in both samples. However, a comparison of the k_{fb} values at equal temperatures for the two samples shows that adsorption is always slower for the surface sample. This suggests that the favoring effect of the proximity is contrasted by changes in the reorientational dynamics. In fact, molecular motions are expected to be more hindered at low levels of hydration.[51]

The desorption mechanism is always expected to be an activated process because it depends on the breaking of the low-energy binding of the molecules to the surface. The temperature dependence of the rate k_{bf} of detachment from the surface is then Arrhenius-like, with an activation energy comparable to the enthalpy of adsorption. The values of the activation energies of desorption of the two samples, derived from the linear fits through the $1/T$ dependences of the logarithm of k_{bf} (Figure 13), are relatively small and comparable (4.8 ± 0.3 kcal mol^{-1} for the sample with volume water and 3.3 ± 0.7 kcal mol^{-1} for the sample with surface water). This seems to be reasonable, as the water phase and the surface are polar media and should not show a greatly different affinity for TA.

The difference in the values of k_{bf} of the two samples at each temperature must be attributed to a different prefactor in the Arrhenius expression. In the framework of the activated complex theory, this means that the desorption activation entropies are different in the two samples, being slightly higher for the sample with volume water than for the other. A lower entropy content of the activated complex in the sample containing surface water may be related to a reduction of the configurations compatible with the total energy. In fact, some orientations and conformations of TA may not be allowed due to the lack of water molecules. This is consistent with the smaller k_{fb} values observed in this sample.

Conclusions

In this paper we have offered some new information about the mechanism of adsorption−desorption of TA molecules in the MCM-41 pores. Results from two samples differing in their water loading (TA in volume water and TA in surface water) were shown. The effects of both the water content and the temperature on the adsorption−desorption parameters follow our general understanding of the molecular binding at the solvent−surface interface in accordance with aspects concerning hindrance of molecular motions and conformers' populations at low levels of hydrations. The dynamic deuterium MAS NMR approach used here can also be applied to many other molecular adsorption−desorption systems, as long as the signal-to-noise ratio is sufficient and a temperature range can be reached where the kinetics is in the order of the deuterium quadrupolar frequencies. Extensions of these studies by using chemical shift anisotropies of spin-half nuclei can also be considered.

We believe that our results contribute to the general effort to understand the behavior of dissolved peptides in contact with surfaces. Although the literature is quite rich in theoretical and experimental studies of the adsorption kinetics of relatively large proteins to solid surfaces,[7,8,52,53] it is surprisingly poor in investigations on oligopeptides. However, oligopeptides could be used as model systems for the more complicated cases of proteins, and a full comprehension of their adsorption−desorption kinetics seems to be necessary.

The present study raises some not trivial questions which have been receiving attention, especially in the recent past. We refer, in particular, to the nature of peptide binding in terms of molecular conformation and number of binding sites, the rotational diffusion and the kinetics of the conformational changes of the molecules, the influence of the water molecules, of the silanols and of the diffusion in solution on the conformational exchange rates. Part of these mechanisms can be studied spectroscopically. For example, the structure of the bound TA molecules as well as water−TA proximity can be studied by NMR using ^{13}C and ^{17}O isotope labeling and exploiting modern correlation spectroscopy, which has already proved to be a powerful tool for determining the secondary structure of surface-adsorbed peptides.[54] A part of these studies is underway in our laboratory.

Acknowledgment. We thank Z. Luz and R. Poupko for helpful discussion and for providing us the program for line shape simulation in the presence of MAS and dynamics. This work was supported by the Center of Excellence "Origin of Ordering and Functionality in Mesostructures hybrid Materials" of the Israel Science Foundation (Grant No. 800301-1). S.P. thanks the Italian National Research Council for partial financial support.

References and Notes

(1) Zaborowski, E.; Zimmermann, H.; Vega, S. *J. Am. Chem. Soc.* **1998**, *120*, 8113−8123.

(2) Geil, B.; Isfort, O.; Boddenberg, B.; Favre, D. E.; Chmelka, B. F.; Fujara, F. *J. Chem. Phys.* **2002**, *116*, 2184−2193.

(3) Shenderovich, I. G.; Buntkowski, G.; Schreiber, A.; Gedat, E.; Sharif, S.; Albrecht, J.; Golubev, N. S.; Findenegg, G.; Limbach, H. H. *J. Phys. Chem. B* **2003**, *107*, 11924−11939.

(4) Hansen, E. W.; Courivaud, F.; Karlsson, A.; Kolboe, S.; Stöcker, M. *Microporous Mesoporous Mater.* **1998**, *22*, 309−320.
(5) Gjerdaker, L.; Aksnes, D. W.; Sørland, G. H.; Stöcker, M. *Microporous Mesoporous Mater.* **2001**, *42*, 89−96.
(6) Stallmach, F.; Graeser, A.; Kärger, J.; Krause, C.; Jeschke, M.; Oberhagemann, U.; Spange, S. *Microporous Mesoporous Mater.* **2001**, *44*−*45*, 745−753.
(7) Malmsten, M. *J. Colloid Interface Sci.* **1998**, *207*, 186−199.
(8) Tie, Y.; Calonder, C.; Van Tassel, P. R. *J. Colloid Interface Sci.* **2003**, *268*, 1−11.
(9) Yang, J.; Daehler, A.; Stevens, G. W.; O'Connor, A. J. *Stud. Surf. Sci. Catal.* **2003**, *146*, 775−778.
(10) Diaz, J. F.; Balkus, K. J., Jr. *J. Mol. Catal. B: Enzymol.* **1996**, *2*, 115−126.
(11) He, J.; Li, X.; Evans, D. G.; Duan, X.; Li, C. *J. Mol. Catal. B: Enzymol.* **2000**, *11*, 45−53.
(12) Takahashi, H.; Li, B.; Sasaki, T.; Miyazaki, C.; Kajino, T.; Inagaki, S. *Microporous Mesoporous Mater.* **2001**, *44*−*45*, 755−762.
(13) Yiu, H. H. P.; Wright, P. A.; Botting, N. P. *Microporous Mesoporous Mater.* **2001**, *44*−*45*, 763−768.
(14) Deere, J.; Magner, E.; Wall, J. G.; Hodnett, B. K. *Catal. Lett.* **2003**, *85*, 19−23.
(15) Barrie, P. J. *Annu. Rep. NMR Spectrosc.* **2000**, *41*, 265−316.
(16) Griffin R. G. In *Methods of Enzymology*; Lowenstein, J. M., Ed.; Academic: New York, 1981; Vol. 72, p 108.
(17) Landau, M. V.; Varkey, S. P.; Herskowitz, M.; Regev, O.; Pevzner, S.; Sen, T.; Luz, Z. *Microporous Mesoporous Mater.* **1999**, *33*, 149−163.
(18) Carpino, L. A.; Han, G. Y. *J. Org. Chem.* **1972**, *37*, 3404−3409.
(19) Chan, W. C.; White, P. D. *Fmoc Solid-Phase Peptide Synthesis: A Practical Approach*; Oxford University Press: Oxford, U.K., 2000.
(20) Bielecki, A.; Burum, D. P. *J. Magn. Reson. A* **1995**, *116*, 215−220.
(21) Luz, Z.; Poupko, R.; Alexander, S. *J. Chem. Phys.* **1993**, *99*, 7544−7553.
(22) Schmidt, A.; Vega, S. *J. Chem. Phys.* **1987**, *87*, 6895−6907.
(23) Conroy, H. *J. Chem. Phys.* **1967**, *47*, 5307−5318.
(24) Bak, M.; Rasmussen, J. T.; Nielsen, N. C. *J. Magn. Reson.* **2000**, *147*, 296−330.
(25) Massiot, D.; Fayon, F.; Capron, M.; King, I.; Le Calvé, S.; Alonso, B.; Durand, J.-O.; Bujoli, B.; Gan, Z.; Hoatson, G. *Magn. Reson. Chem.* **2002**, *40*, 70−76.
(26) Bronnimann, C. E.; Zeigler, R. C.; Maciel, G. E. *J. Am. Chem. Soc.* **1988**, *110*, 2023−2026.
(27) Schreiber, A.; Ketelsen, I.; Findenegg, G. H. *Phys. Chem. Chem. Phys.* **2001**, *3*, 1185−1195.
(28) Grünberg, B.; Emmler, T.; Gedat, E.; Shenderovich, I.; Findenegg, G. H.; Limbach, H. H.; Buntkowsky, G. *Chem. Eur. J.*, submitted.
(29) Zhao, X. S.; Lu, G. Q.; Whittaker, A. K.; Millar, G. J.; Zhu, H. Y. *J. Phys. Chem. B* **1997**, *101*, 6525−6531.
(30) Cauvel, A.; Brunel, D.; Di Renzo, F.; Garrone, E.; Fubini, B. *Langmuir* **1997**, *13*, 2773−2778.
(31) Anwander, R.; Nagl, I.; Widenmeyer, M.; Engelhardt, G.; Groeger, O.; Palm, C.; Röser, T. *J. Phys. Chem. B* **2000**, *104*, 3532−3544.
(32) Hansen, E. W.; Schmidt, R.; Stöcker, M.; Akporiaye, D. *J. Phys. Chem.* **1995**, *99*, 4148−4154.
(33) Matthae, F. P.; Basler, W. D.; Lechert, H. In *Mesoporous Molecular Sieves 1998;* Bounneviot, L., Béland, F., Danumah, C., Giasson, S., Kaliaguine, S., Eds.; Studies in Surface Science and Catalysis 117; Elsevier: Amsterdam, 1998; pp 301−308.
(34) Bloembergen, N.; Purcell, E. M.; Pound, R. V. *Phys. Rev.* **1948**, *73*, 679−712.
(35) Hansen, E. W.; Schmidt, R.; Stöcker, M.; Akporiaye, D. *Microporous Mater.* **1995**, *5*, 143−150.
(36) Takahara, S.; Nakano, M.; Kittaka, S.; Kuroda, Y.; Mori, T.; Hamano, H.; Yamaguchi, T. *J. Phys. Chem. B* **1999**, *103*, 5814−5819.
(37) Stallmach, F.; Kärger, J.; Krause, C.; Jeschke, M.; Oberhagemann, U. *J. Am. Chem. Soc.* **2000**, *122*, 9237−9242.
(38) Yu, T. Y.; Cheng, C. Y.; Hwang, D. W.; Huang, H. W.; Hwang, L. P. *Appl. Magn. Reson.* **2000**, *18*, 435−453.
(39) Hwang, D. W.; Sinha, A. K.; Cheng, C. Y.; Yu, T. Y.; Hwang, L. P. *J. Phys. Chem.* **2001**, *105*, 5713−5721.
(40) Chen, L.; Gross, T.; Lüdemann, H. *Z. Naturforsch.* **2000**, *55a*, 473−477.
(41) Smirnov, P.; Yamaguchi, T.; Kittaka, S.; Takahara, S.; Kuroda, Y. *J. Phys. Chem. B* **2000**, *104*, 5498−5504.
(42) Eckert, H.; Yesinowski, J. P.; Stolper, E. M. *Solid State Ionics* **1989**, *32/33*, 298−313.
(43) Peri, J. B. *J. Phys. Chem.* **1966**, *70*, 2937−2945.
(44) Dill, K. A. *Protein Sci.* **1999**, *8*, 1166−1180.
(45) Eker, F.; Griebenow, K.; Schweitzer-Stenner, R. *J. Am. Chem. Soc.* **2003**, *125*, 8178−8185.
(46) Schweitzer-Stenner, R.; Eker, F.; Griebenow, K.; Cao, X.; Nafie, L. A. *J. Am. Chem. Soc.* **2004**, *126*, 2768−2776.
(47) Mittermaier, A.; Kay, L. E. *J. Am. Chem. Soc.* **1999**, *121*, 10608−10613.
(48) Burnett, L. H.; Muller, B. H. *J. Chem. Phys.* **1971**, *55*, 5829−5831.
(49) Ottinger, M.; Bax, A. *J. Am. Chem. Soc.* **1999**, *121*, 4690−4695.
(50) Langmuir, I. *J. Am. Chem. Soc.* **1918**, *40*, 1361−1403.
(51) Rupley, J. A.; Careri, G. *Adv. Protein Chem.* **1991**, *41*, 37−172.
(52) Schaaf, P.; Voegel, J. C.; Senger, B. *J. Phys. Chem. B* **2000**, *104*, 2204−2214.
(53) Brusatori, M. A.; Van Tassel, P. R. *J. Colloid Interface Sci.* **1999**, *219*, 333−338.
(54) Long, J. R.; Oyler, N.; Drobny, G. P.; Stayton, P. S. *J. Am. Chem. Soc.* **2002**, *124*, 6297−6303.